Check for updates

AGU Advances

RESEARCH ARTICLE
10.1029/2023AV001151

Escalating Wildfires in Siberia Driven by Climate Feedbacks Under a Warming Arctic in the 21st Century

Xin Huang[1,2], Lian Xue[1], Zilin Wang[1], Yawen Liu[1], Ke Ding[1], and Aijun Ding[1,2]

[1]School of Atmospheric Sciences, Nanjing University, Nanjing, China, [2]Frontiers Science Center for Critical Earth Material Cycling, Nanjing University, Nanjing, China

Xin Huang and Lian Xue contributed equally to this work.

Peer Review The peer review history for this article is available as a PDF in the Supporting Information.

Key Points:

- A warm-dry weather condition aggravates wildfire severity over Siberia in the past two decades
- Smoke aerosols emitted from wildfires suppress the precipitation via aerosol-cloud interaction, forming a self-amplifying feedback loop in Siberia

Supporting Information:

Supporting Information may be found in the online version of this article.

Correspondence to:

X. Huang,
xinhuang@nju.edu.cn

Citation:

Huang, X., Xue, L., Wang, Z., Liu, Y., Ding, K., & Ding, A. (2024). Escalating wildfires in Siberia driven by climate feedbacks under a warming Arctic in the 21st century. *AGU Advances*, *5*, e2023AV001151. https://doi.org/10.1029/2023AV001151

Received 15 DEC 2023
Accepted 2 AUG 2024

Author Contributions:
Conceptualization: Xin Huang, Aijun Ding
Data curation: Ke Ding
Formal analysis: Xin Huang, Lian Xue
Funding acquisition: Xin Huang, Aijun Ding
Investigation: Xin Huang
Methodology: Xin Huang, Lian Xue
Project administration: Aijun Ding
Resources: Lian Xue
Software: Xin Huang
Validation: Xin Huang, Lian Xue

© 2024. The Author(s).
This is an open access article under the terms of the Creative Commons Attribution-NonCommercial-NoDerivs License, which permits use and distribution in any medium, provided the original work is properly cited, the use is non-commercial and no modifications or adaptations are made.

Abstract

Siberian wildfire is of paramount importance in the carbon cycle and climate change as it is a major disturbance in the pan-Arctic ecosystems. In recent decades, the Siberian wildfire regime has been shifting; however, less is known about its process-based feedback mechanisms. By integrating in-situ and satellite observational data sets as well as chemistry-climate coupled modeling, we find that central Siberia has featured the most prominent wildfire escalation during the past two decades, which is closely related to hydrological drought with decreasing rainfall and drying soil under a fast-warming Arctic. Furthermore, fire-emitted aerosols compound the increasing wildfires via serving as cloud condensation nuclei and suppressing precipitation, forming self-amplifying feedback. As the Arctic warming is projected to continue, wildfires are estimated to more than double by the end of this century. This work highlights the great importance of fire risk management based on a fundamental scientific understanding of the complex climate system.

Plain Language Summary

Wildfire, a major disturbance in terrestrial ecosystems, is of paramount importance in climate change, especially in high latitudes. Siberian wildfire has been escalating since the onset of this century, with fast-increasing burned area as well as poleward expansion. We demonstrate that such a wildfire escalation is closely related to a warming Arctic, which suppresses precipitation and aggravates hydrological drought in central Siberia. Besides, fire smoke could trigger self-amplifying feedback via aerosol-cloud interaction, further compounding Siberian wildfires. This work identifies the escalating wildfire risk in central Siberia and the main drivers. As the Arctic is projected to be further warmed by the end of this century, the urgency of risk management and fire-climate adaptation in Siberia is underscored.

1. Introduction

Boreal and Arctic terrestrial ecosystems have been serving as a carbon sink and are critically important in the global climate system (Pan et al., 2011; Schuur et al., 2015). Arctic permafrost, storing nearly 1,700 billion metric tons of frozen and thawing carbon, is one of the world's largest carbon reservoirs. It is estimated that permafrost carbon reservoirs approximately double the global atmospheric carbon (Hugelius et al., 2014; Miner et al., 2022). However, pan-Arctic wildfires, including peatland and boreal forest burning, would shift Arctic and boreal lands from carbon sinks to carbon sources via direct combustion emission as well as disrupting vegetation regeneration (Bond-Lamberty et al., 2007; Descals et al., 2022; Song et al., 2019; Walker et al., 2019; Zheng et al., 2021). Furthermore, recent study has demonstrated that wildfires are also intricately linked with permafrost degradation because the combustion of vegetation and soil carbon would warm permafrost and increase microbial respiration that even releases ancient carbon into the atmosphere (J. Huang et al., 2017). Across the pan-Arctic area, Siberian wildfire occurrence and severity have drawn great attentions and have been predicted to increase in the upcoming decades with severe negative impacts (Chen et al., 2021).

It is worth noting that wildfires are highly sensitive to climate change, which are dominant large-scale drivers of shaping fire-prone landscapes and determining fire behaviors (Abatzoglou et al., 2021; Bessie & Johnson, 1995; Scholten et al., 2022). Increasing carbon emissions from both wildfires and fossil fuel combustion in some regions during past decades have been compounding global warming (Brown et al., 2023; Mekonnen et al., 2022). The Arctic warming is emerging as a scientific and societal concern because the warming trend in this region is found to be 2–4 times faster than that of the rest of the world over the past 30 years, which is also known as Arctic amplification (Francis et al., 2017; Post et al., 2019). The warming trend of climate has been found to exacerbate wildfires via rising air temperature, deepening drought and suppressing precipitation, thereby making vegetation greatly combustible and driving rapid fire spread (Y. Liu et al., 2010; Westerling et al., 2006). In comparison to

Visualization: Xin Huang, Lian Xue
Writing – original draft: Xin Huang, Lian Xue
Writing – review & editing: Xin Huang, Lian Xue, Zilin Wang, Yawen Liu, Aijun Ding

other wildfire-prone regions, Siberia is exceptionally vulnerable to Arctic climate warming and wildfire intensification is far more severe because the carbon-rich soil could become highly flammable as high air temperature thaw and dry the permafrost (McCarty et al., 2020; Rein & Huang, 2021). In recent years, wildfires across Siberia have been unprecedented, with large and more severe fires sparking global concern (Mccarty et al., 2021; Talucci et al., 2022). An obvious increase in fire severity and lengthening of fire season since the beginning of the century has been detected in Siberia with a positive air temperature trend (Tomshin & Solovyev, 2021). Apart from the decades-long warming trend, recent studies also indicated that climate variability at different time scales could also influence the wildfire intensities over the pan-Arctic region, including North Atlantic Oscillation, Arctic Oscillation, and East Atlantic pattern (Kim et al., 2020; Marquardt Collow et al., 2022; Zhu et al., 2021).

More than merely being responsive to climate change, wildfire in turn influences climate by releasing heat-trapping greenhouse gases into the atmosphere (Irannezhad et al., 2020), plausibly contributing to positive carbon-climate feedback. Even worse, wildfire-emitted smoke that contains a large amount of light-absorbing carbonaceous aerosols, including black carbon and organic aerosol (Giglio et al., 2013; Yu et al., 2019), has been demonstrated to substantially influence thermal and humidity conditions, atmospheric stability, and precipitation, in some cases giving rise to a positive fire-smoke-weather feedback (X. Huang et al., 2023; Kochanski et al., 2019; Lu et al., 2018; Petäjä et al., 2016). In the high latitudes, the climatic feedback of wildfire smoke is particularly complex (Baklanov et al., 2021). Fire-emitted carbonaceous aerosols not only perturb the radiation balance (Petäjä et al., 2022), but also modify cloud properties and deposit on the glacier surface (Aubry-Wake et al., 2022), leading to a longer dry season and providing greater opportunities and frequency for extremely large fires. Therefore, the complex feedback and interactions between wildfires and climate are great challenges that we face in understanding and managing fire risk, especially in climate-sensitive regions like Siberia.

Multiple lines of evidences have indicated that Siberian wildfire is greatly modulated by climate change and is currently intensifying under a fast-warming Arctic (Kirillina et al., 2020; McCarty et al., 2020; Piao et al., 2020). However, the climatic drivers, underlying feedbacks/interactions ongoing in the Arctic and future risk of Siberian wildfires still need to be thoroughly explored and comprehensively assessed. Here, by integrating 20-year ground-based and satellite observations of wildfires and meteorology, atmospheric reanalysis data together with climate-chemistry coupled modeling, we explore the primary driving forces and the climate feedback of the escalating Siberian wildfire and its plausible linkage with the fast-warming Arctic. On the basis of mechanism understanding, the wildfire risk in Siberia by the end of this century is assessed according to climate projection under typical shared socioeconomic pathways (SSP) within the Coupled Model Intercomparison Project Phases 6 (CMIP6).

2. Materials and Methods

2.1. Wildfire Data Sets and Satellite Observations

The Moderate Resolution Imaging Spectroradiometer (MODIS) onboard the Terra and Aqua satellites has been monitoring fires since the year 2001, and the thermal anomalies and fire product (MOD14A1 and MYD14A1) provides the location and timing of the fires globally. The Terra and Aqua combined MCD64A1 Burned Area data product is a monthly, global gridded 500-m product containing per-pixel burned-area and quality information. The MCD64A1 burned-area mapping approach employs MODIS Surface Reflectance imagery coupled with 1 km (km) MODIS active fire observations (Wiedinmyer et al., 2011). Since MODIS fire products might double-count the same fire that occurs on a single day, we used burned-area derived by The Fire Inventory from NCAR (FINN version 1.5), which removes fire detections that fall within a 1 km^2 radius of another fire detection on a daily basis. Therefore, for each 1 km^2 hot spot, there can be only one fire per day (Wiedinmyer et al., 2011). FINN model provides daily high-resolution burned area and emissions of wildfire at a horizontal resolution of 1 km × 1 km. The burned area data during the time period from 2002 to 2021 is used in this study. To validate the performance of FINN burned area used in this work, we also include the Global Fire Emissions Database (GFED) data for comparisons, which combines satellite information on fire activity and vegetation productivity to estimate gridded monthly burned area and fire emissions (Wiedinmyer et al., 2011). We compare these fire detections from different products/data sets, including MCD64A1 burned area, FINN burned area and Global Fire Emissions Database (GFED, Version 4.1) carbon emission data set. As shown in Figure S3 in Supporting Information S1, all the data set shows similar interannual variability and increasing trends in central Siberian wildfires.

2576604x, 2024, 4, Downloaded from https://agupubs.onlinelibrary.wiley.com/doi/10.1029/2023AV001151 by Nanjing University, Wiley Online Library on [11/09/2024]. See the Terms and Conditions (https://onlinelibrary.wiley.com/terms-and-conditions) on Wiley Online Library for rules of use; OA articles are governed by the applicable Creative Commons License

To demonstrate the horizontal and vertical structure of aerosol and cloud, MODIS monthly aerosol optical depth and cloud fraction retrievals (MOD08 and MOD06) during 2002–2021 and Cloud-Aerosol Lidar and Infrared Pathfinder Satellite Observations (CALIPSO, level 3 aerosol profile product) that provides information on vertical distributions of smoke extinction and cloud since 2007 are also employed. Permafrost extent in the Northern Hemisphere with a spatial resolution of around 1 km is obtained from Permafrost data products from the European Space Agency's Climate Change Initiative Permafrost project (ESACCI, version 3.0) for the period 1997–2019 (Obu et al., 2021).

2.2. Atmospheric Reanalysis Data and Meteorological Observations

Historical meteorologic parameters since the year 2002 are acquired from the fifth generation of European Centre for Medium-Range Weather Forecasts (ECMWF) ERA5 reanalysis data. ERA5 reanalysis data provides hourly estimates of a large number of atmospheric, land, and oceanic climate variables, which are produced using data assimilation and model forecasts of the ECMWF Integrated Forecast System (IFS), with a horizontal resolution of $0.25° \times 0.25°$ and 137 hybrid levels from the surface up to a height of approximately 80 km. Here, hourly reanalysis data of 2-m air temperature, 2-m relative humidity, 10-m wind speed, rainfall rate, soil water content at the surface, and wind and cloud at different pressure levels during the time period from 2002 to 2021 are utilized to investigate the climatic conditions and their variabilities in the pan-Arctic region. The surface weather observations data set (TD3505 Integrated Surface Hourly Data), which consists of 2-m temperature and wind observations at over 10,000 globally distributed stations, is employed to demonstrate the temperature variability in the study domain. In this work, we obtained the hourly air temperature observations archived at the National Climatic Data Center (NCDC) to calculate the observed temperature trend in Siberia.

2.3. Climate-Chemistry Coupled Modeling

To investigate the climate feedback of fire smoke aerosol, we conducted sensitivity simulations using the Community Atmosphere Model Version 6 (CAM6) with chemistry of the National Center for Atmospheric Research (NCAR) Community Earth System Model (CESM version 2.1.0) (Danabasoglu et al., 2020). New chemical and physical representations of direct and indirect aerosol effects and their interactions with clouds are among the improvements made by the CAM6. Meanwhile, a default of the Modal Aerosol Model version 4 (MAM4) with improved treatment of aerosols has been implemented (X. Liu et al., 2016). Additional updates include the Morrison-Gettelman cloud microphysics scheme, aerosol-temperature-dependent mixed-phase ice nucleation, a unified turbulence scheme for different cloud types. The CESM2 has been identified as one of the most skillful models that could well represent the present climate status (Fukutomi et al., 2004). In this study, two parallel simulations, BASE run and noBB (biomass burning) run, have been performed at $0.9° \times 1.25°$ horizontal grids with 32 vertical levels. Both tests were conducted for 10 years to gain a balanced climatological state of 2010s after a 1-year spin-up. All emission inventories implemented are from the data set representing the climatological status in the 2010s developed for assessments in the CMIP6(Hoesly et al., 2018; Van Marle et al., 2017), and have been re-gridded to the model grids. The aforementioned two simulations share exactly the same model configurations and anthropogenic emission inventories, while only differ from each other in biomass burning emission input. Specifically, the BASE run used the historical global biomass burning emissions for CMIP6 (Van Marle et al., 2017), averaging between 2006 and 2014 and cycling for every model year, whereas the noBB run excluded the biomass burning emissions. The difference between the output results from the two simulations has then been regarded as the meteorological response to the wildfire emissions.

2.4. Fire Weather Index Calculation

The fire weather index (FWI) is capable of indicating fire intensity by combining weather factors influencing the likelihood of a vegetation fire starting and spreading with the amount of fuel being consumed (Van Wagner, 1987). Here, to investigate the impact of fire-emitted aerosols on rainfall and thus the fire risk probability, FWI is calculated using the Canadian Forest Service Fire Weather Index rating system (FWI) given the fact that this index has been proven to have a good correlation with the Siberian wildfire (Jones et al., 2022). The calculation procedures for FWI could be summarized into three main steps. First, three fuel moisture codes are calculated based on 2-m temperature, 2-m relative humidity, 10-m wind speed, and 24-hr accumulated precipitation. Then, the Initial Spread Index (ISI) and Build-up Index (BUI) are derived from these codes to represent fire spread rate and fuel dryness. Finally, the FWI combines ISI and BUI into a unitless index indicating peak

2576604x, 2024, 4, Downloaded from https://agupubs.onlinelibrary.wiley.com/doi/10.1029/2023AV001151 by Nanjing University, Wiley Online Library on [11/09/2024]. See the Terms and Conditions (https://onlinelibrary.wiley.com/terms-and-conditions) on Wiley Online Library for rules of use; OA articles are governed by the applicable Creative Commons License

2576604x, 2024, 4, Downloaded from https://agupubs.onlinelibrary.wiley.com/doi/10.1029/2023AV001151 by Nanjing University, Wiley Online Library on [11/09/2024]. See the Terms and Conditions (https://onlinelibrary.wiley.com/terms-and-conditions) on Wiley Online Library for rules of use; OA articles are governed by the applicable Creative Commons License

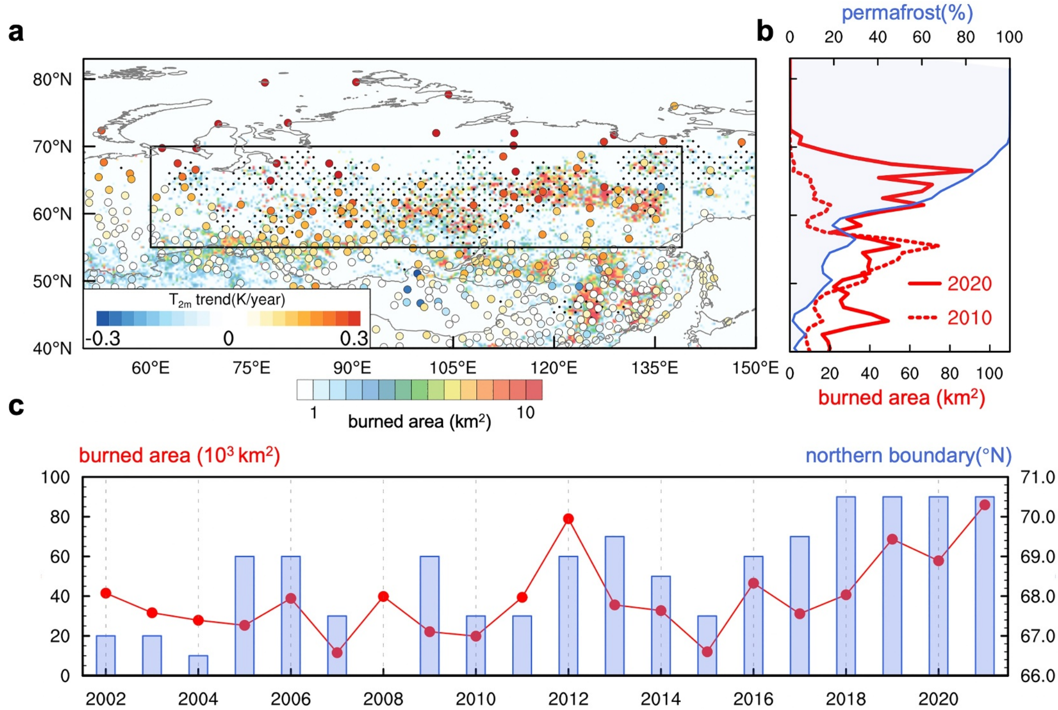

Figure 1. Siberian wildfire and warming trend in the past two decades. (a) Map showing FINN burned area of wildfires and observed 2-m air temperature (T_{2m}) trend during 2002–2021. The black dots mark the locations where the wildfire burned areas have more than doubled in the past two decades. The black rectangle marks the study domain of this work. (b) Zonal averaged (60–140°E) permafrost coverage and wildfire burned area in 2010 and 2020. (c) Northern boundary of large fires (zonal aggregated burned area greater than 100 km^2) and burned area of wildfires in central Siberia (black rectangle in (a)) from 2002 to 2021.

daily fire risk (Van Wagner, 1987). Given that the summertime rainfall can be influenced by the fire-emitted aerosol, we calculated the FWI based on the meteorological data from experiments BASE and noBB. The initial FWI condition is the climatology mean of FWI in July during 2011–2020 obtained from gridded fire danger forecast products from the global ECMWF Fire Forecast.

3. Results

3.1. Arctic Warming and Escalating Siberian Wildfire

Periodic wildfires are a permanent natural process of Siberian coniferous forests mainly consisting of larch, spruce, and pine, most of which are underlain by vast deposits of carbon-rich soil (Figures S1 and S2 in Supporting Information S1). Different from other biomass-burning regions, Siberian wildfires not only burn the surface vegetation, but also consume the organic soil, feeding large-size and long-duration fires with an enormous amount of fuel (Rein, 2013). High-latitude wildfires, especially those above the Arctic Circle (north of 67°N), predominately concentrate to the east of Ural Mountains and to the west of Verkhoyansk Ranges (55–70°N, 60–140°E, hereafter called central Siberia, indicated by the black rectangle in Figure 1a and Figure S2 in Supporting Information S1). In the past 20 years, wildfire activities in central Siberia have more than doubled according to satellite-derived burned area estimation from both Moderate Resolution Imaging Spectroradiometer (MODIS) MCD64A1 Burned Area data product and Fire Inventory from National Center for Atmospheric Research (FINN) burned area estimation (Figure S3 in Supporting Information S1). The zonal-aggregated burned area of wildfire has increased from less than 40,000 km^2 in the early 2000s to ~80,000 km^2 in the 2020s (Figure 1c), corresponding to the recent findings that Siberian wildfires are getting clustered and intensified (Masrur et al., 2018; Tomshin & Solovyev, 2021). Spatially, the region with the most prominent wildfire escalation features a substantial warming tendency in the past two decades, especially the area north of 60°N (Figure 1a).

Such a drastic enhancement in wildfire activities in central Siberia is also well demonstrated by fire carbon emissions. Quantitatively, the carbon emission estimation in central Siberia (black rectangle in Figure 1a) derived from the Global Fire Emissions Database (GFED) soared from 22.9 Mt Carbon in 2000 to 351.5 Mt Carbon in 2020 (Giglio et al., 2013) (Figure S3 in Supporting Information S1). Aside from the doubled burned area of wildfire in central Siberia, such a dramatic increase in carbon emission is also attributed to the spatial redistribution of wildfire activities. Satellite fire detection clearly demonstrates that the Siberian fire regimes have undergone substantial shifts. As illustrated in Figure 1b and Figure S2 in Supporting Information S1, wildfires in central Siberia have been expanding northward and poleward in the past two decades. At the beginning of the 21st Century, large fires (zonal aggregated burned area greater than 100 km^2) in central Siberia mostly occurred around 67°N and farther south, and hardly can large fires scorch north of 70°N. However, wildfires have reached north of 70°N almost every single year since 2018, leading to unprecedented wildfires in the Arctic Circle. Smoke from wildfires raging in Siberia has even reached the North Pole in historic first in August 2021 (Figure S4 in Supporting information S1) (Zheng et al., 2023). Such a poleward wildfire expansion would expose an increasing permafrost and the associated huge carbon reservoir to ravaging wildfires (Figure 1b). By combining the FINN burned area data set and permafrost distribution derived from the European Space Agency's Climate Change Initiative Permafrost project (ESACCI, version 3) (Obu et al., 2021), we estimate that the area of permafrost subjective to wildfires has increased by 75% in the past decade. Quantitatively, the area of permafrost exposed to wildfire in central Siberia during 2002–2011 was 161,472 km^2, while the corresponding value for 2012–2021 was as high as 282,213 km^2, further unlocking the huge soil carbon.

3.2. Impact of Warming-Induced Drought on Siberian Wildfire

Seasonally, Siberia is generally subjected to intense wildfires from April to October as surface temperature gets warm and the snow line retreats (Talucci et al., 2022). Generally, summer (June–August) features the most vigorous wildfire activities in central Siberia (Figure 2a), and it also marks the season with the most significant expansion and intensification of wildfires (Figure S5 in Supporting Information S1). In this region, climatic conditions, like air temperature and precipitation, have been attributed as drivers modulating the interannual variability of wildfire frequency and intensity (Smith et al., 2021; Xing et al., 2017). To identify the key factors modulating central Siberian wildfires, we collected multiple meteorological parameters from the state-of-the-art atmospheric reanalysis data (ERA5) during 2002–2021, including near-surface air temperature, relative humidity, wind, soil moisture, and rainfall. Figure 2a indicates that rainfall and soil moisture dominate the interannual wildfire variations in summer and autumn, corroborating that warmer histosols with higher moisture deficiency are key factors creating and accelerating the ignition and spread of fires in this region (Bartsch et al., 2009; Rein & Huang, 2021).

During the summertime when the wildfires are most intensive and feature the fastest intensification, the correlation coefficient of fire burned area on soil moisture could reach up to −0.7. Such a significant negative relationship also holds true on a daily basis over central Siberia in the past two decades. It is worth noting that air temperature and soil moisture in summer during the past two decades are anti-correlated virtually. In statistical terms, warm dry periods coincide with the majority of wildfire occurrences (Figure S6 in Supporting Information S1), plausibly via boosting the readiness of vegetation and soil to burn. Figure 2b clearly indicates that the summertime soil moisture has been descending with a rising air temperature since the beginning of the 21st century. One exception was the anomalously hot summer of 2012 when the soil was quite dry, and the burned area in central Siberia peaked around 67,000 km^2. This exactly proves how important the warming climate might be in Siberian wildfires. As the Arctic climate warms up, in 2019–2021 when surface soil moisture was dried down to ~345 kg m^{-3}, burned areas of central Siberian wildfire were more than twice the 20-year average of 27,000 km^2, readily hitting the peak in climatically anomalous year 2012. The great importance of hydrological drought in fostering wildfire and its close linkage with air temperature raises the question of how the warming climate impacts Siberian wildfires.

By analyzing daily meteorological conditions from 20-year reanalysis data, we found that such a prominent drop of soil moisture in central Siberia is closely related to less rainfall under a rapidly warming Arctic. As the direct driver of soil water storage, summertime precipitation has been receding over central Siberia (Figure 3), with a regional average trend of −0.2 mm/year. There are two main causes for less precipitation and both are linked with Arctic warming. On one hand, the substantial warming would certainly lead to a decrease in relative humidity, lowering precipitable water in the atmosphere (Figures 3a and 3b). Over the Siberian Plateau, where the air

2576604x, 2024, 4, Downloaded from https://agupubs.onlinelibrary.wiley.com/doi/10.1029/2023AV001151 by Nanjing University, Wiley Online Library on [11/09/2024]. See the Terms and Conditions (https://onlinelibrary.wiley.com/terms-and-conditions) on Wiley Online Library for rules of use; OA articles are governed by the applicable Creative Commons License

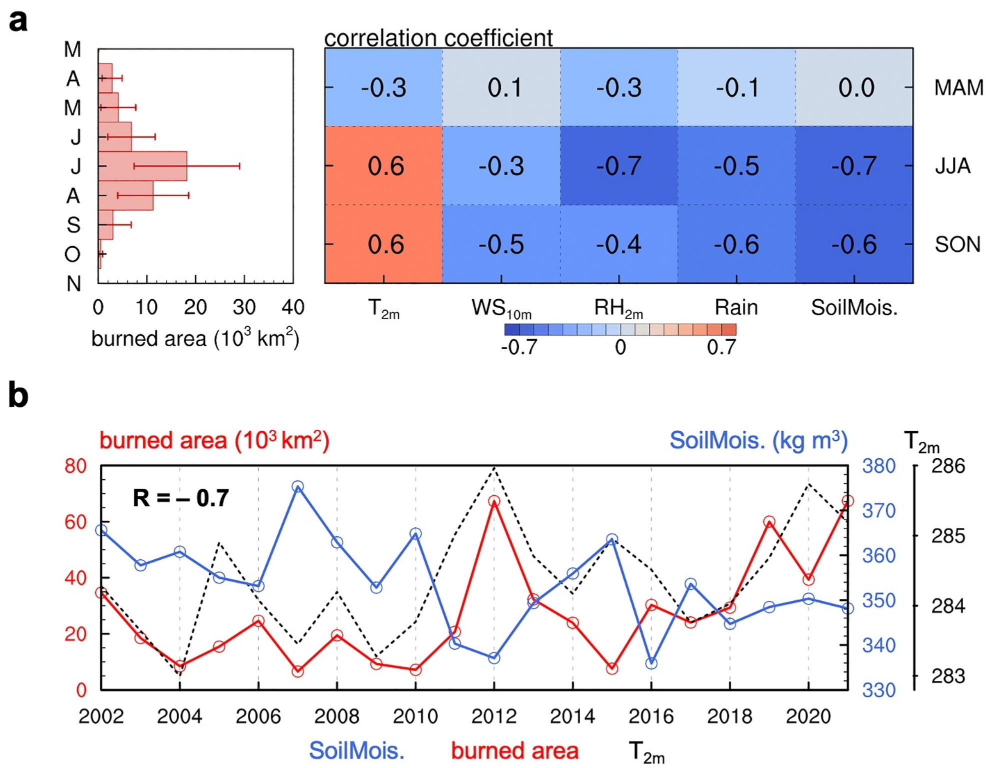

Figure 2. Relationship between wildfire and meteorology in central Siberia in different seasons. (a) Seasonality of burned area of central Siberian wildfires averaged for 2002–2021 (left panel). Stand deviations are shown by whiskers. A correlation coefficient plot between seasonal wildfire burned areas in central Siberia (black rectangle in Figure 1a) and various meteorological parameters in the past two decades (right panel), including 2-m air temperature (T_{2m}), 10-m wind speed (WS_{10m}), 2-m relative humidity (RH_{2m}), rainfall rate (Rain), and surface soil moisture (SoilMois.). (b) Interannual variability of central Siberian wildfires, 2-m air temperature and soil moisture in summer during 2002–2021. The correlation coefficient of fire burned area and soil moisture is labeled in the top left corner.

temperature warmed by approximately 0.08 K/year, the decrease in relative humidity could reach up to ∼0.2%/year at an 850-hPa altitude where the rain clouds gather. On the other hand, changes in large-scale circulation and storm tracks associated with Arctic warming also play a vital role in Siberian precipitation in summer. It is well acknowledged that, over northern Eurasia, the establishment of the mid-summer precipitation belt is largely supported by the regional storm track activities, characterized by high-frequency transient eddies (Fukutomi et al., 2004; Serreze et al., 2003) and mediated by the Arctic polar jet (Xu et al., 2019). The 20-year trend of mean standard deviation (SD) of 10-day high-pass filtered daily 500-hPa geopotential height and 300-hPa meridional wind, which is the indicator for the intensity of synoptic-scale eddy activity, exhibits clear declining signals at 55°N–70°N (Figure S7 in Supporting Information S1), consistent with the northward shifting of the Arctic polar jet (Scholten et al., 2022). Accordingly, the transient eddy meridional moisture flux (see Text in Supporting Information S1), which represents the moisture transport by synoptic-scale storms and largely contributes to the precipitation over Siberia (Fukutomi et al., 2004), has been decreasing during the past two decades with a rate of exceeding −0.5 g kg^{-1}/year over the Siberian Plateau (Figure 3c). Such weakening summer storm tracks in Siberia is closely linked with the warming Arctic, since that the reduced low-level baroclinicity associated with the decreasing poleward temperature gradients could diminish synoptic-scale cyclogenesis and then weaken the storm tracks (Coumou et al., 2015; Hoskins & Woollings, 2015; Nitzbon et al., 2020). As a result, the strong reductions in soil water availability associated with less precipitation could lead to higher fire danger in central Siberia in summer.

3.3. Amplified Siberian Wildfire by Smoke Aerosols-Cloud Interaction

The rising wildfire in central Siberia is expected to release an increasingly large quantity of smoke aerosols into the atmosphere (Figure S8 in Supporting Information S1) (Guan et al., 2020), which may in turn play a role in fire

2576604x, 2024, 4, Downloaded from https://agupubs.onlinelibrary.wiley.com/doi/10.1029/2023AV001151 by Nanjing University, Wiley Online Library on [11/09/2024]. See the Terms and Conditions (https://onlinelibrary.wiley.com/terms-and-conditions) on Wiley Online Library for rules of use; OA articles are governed by the applicable Creative Commons License

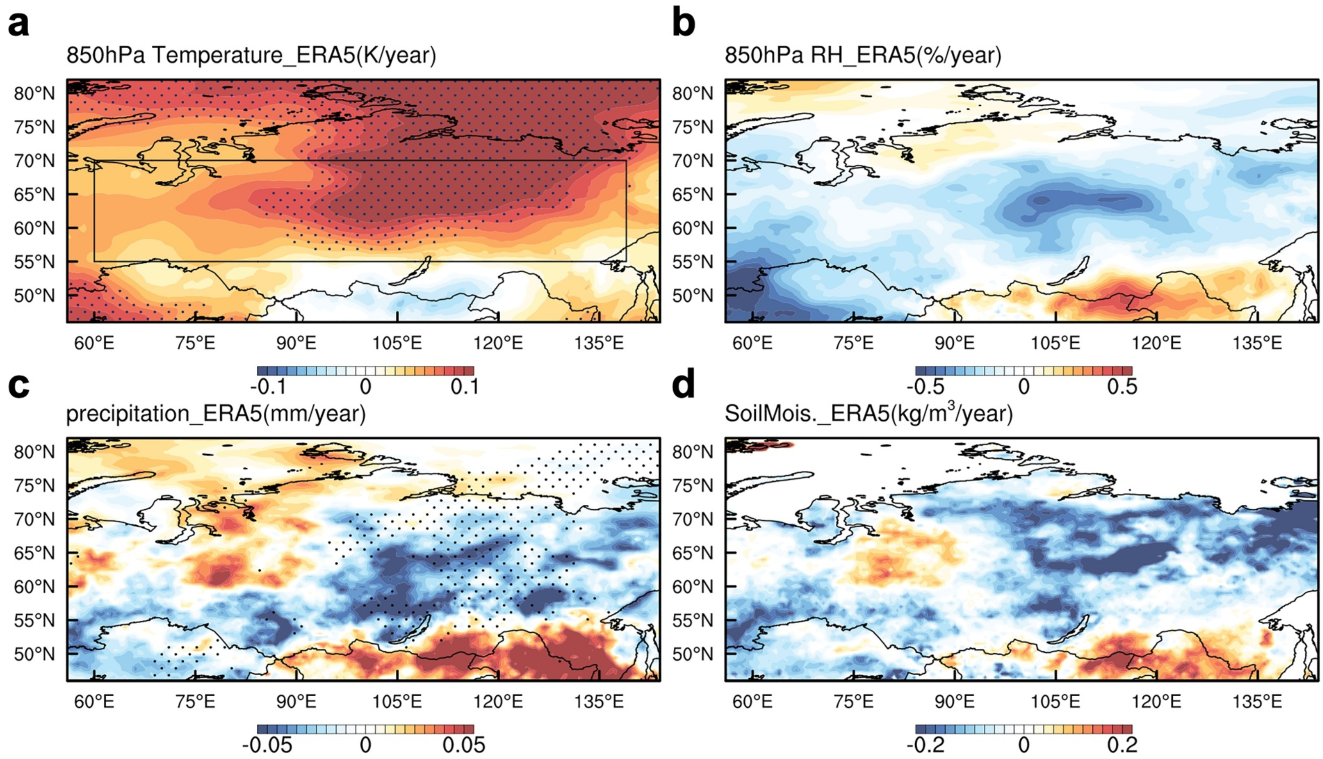

Figure 3. Arctic warming decreases summertime soil moisture in central Siberia in the past two decades. (a) Summertime 850-hPa air temperature trend derived from ERA5 reanalysis data during 2002–2021. Areas with a significant warming tendency ($p > 0.9$) are marked by black dots. (b) Summertime trend of relative humidity (RH) at 850 hPa. (c) Spatial distribution of trend in summertime precipitation. Black dots indicate areas with a decreasing trend greater than -0.5 g kg^{-1}/year in transient meridional moisture flux at 850–925 hPa. (d) Map showing soil moisture (SoilMois.) trend during the past two decades.

weather conditions. It is worth noting that, in the past two decades, the cloud radius observed by MODIS in this region also shows a declining tendency and is virtually anti-correlated with aerosol optical depth (AOD), with a correlation coefficient of −0.65. As shown in Figure 4a, during fire-intensive years (2012, 2019 and 2021), the regional-averaged summertime AOD observations could reach up to 0.42, whereas the corresponding value is as low as 0.20 during low-fire intensity years (2007, 2009, and 2010). Accordingly, the observed cloud droplet radius is relatively smaller during the fire-intensive summers. In spatial, the regions with higher AOD values also feature significant decreases in cloud radius (Figures 4b and 4c), and coincide with dense wildfire emissions. Multiple studies have proven that smoke aerosols can pose feedback to the climate system via directly perturbating radiation transfer (aerosol-radiation interaction) or indirectly serving as cloud condensation nuclei (CCN) and modifying the cloud microphysics properties (aerosol-cloud interactions) (Gao et al., 2018; Schill et al., 2020). In central Siberia, such feedback between wildfire and regional climate might be of importance in increasing wildfire activities. To quantitatively understand the role of smoke aerosols on climate, we performed numerical simulations using the state-of-the-art climate-chemistry coupled model Community Earth System Model (CESM, see Materials and Methods) for the climatological run of the 2010s. Multiple observational data sets were collected to validate the model performance of representing climate and pollution conditions (Figures S9–S11 in Supporting Information S1).

Unlike other biomass-burning regions, in Siberia where smoldering combustion of boreal forest and tundra consume a large proportion of biomass (Hu et al., 2018), carbonaceous aerosol emission from wildfire is exceptionally pronounced and overwhelms that from anthropogenic activities (Figure S8 in Supporting Information S1). The sensitivity simulations clearly show that the emission-intensive Siberian wildfires have given rise to summertime haze pollution over the high-northern-latitude region, with the smoke plume stretching from 60°E to 150°E. Such a high aerosol-containing pollution belt is overlapped with thick low clouds (Figure S11a in Supporting Information S1). Since that the liquid water content of clouds in Siberia is CCN limited and is highly sensitive to aerosol concentrations (Stevens et al., 2018), such a soaring aerosol loading could significantly

2576604x, 2024, 4, Downloaded from https://agupubs.onlinelibrary.wiley.com/doi/10.1029/2023AV001151 by Nanjing University, Wiley Online Library on [11/09/2024]. See the Terms and Conditions (https://onlinelibrary.wiley.com/terms-and-conditions) on Wiley Online Library for rules of use; OA articles are governed by the applicable Creative Commons License

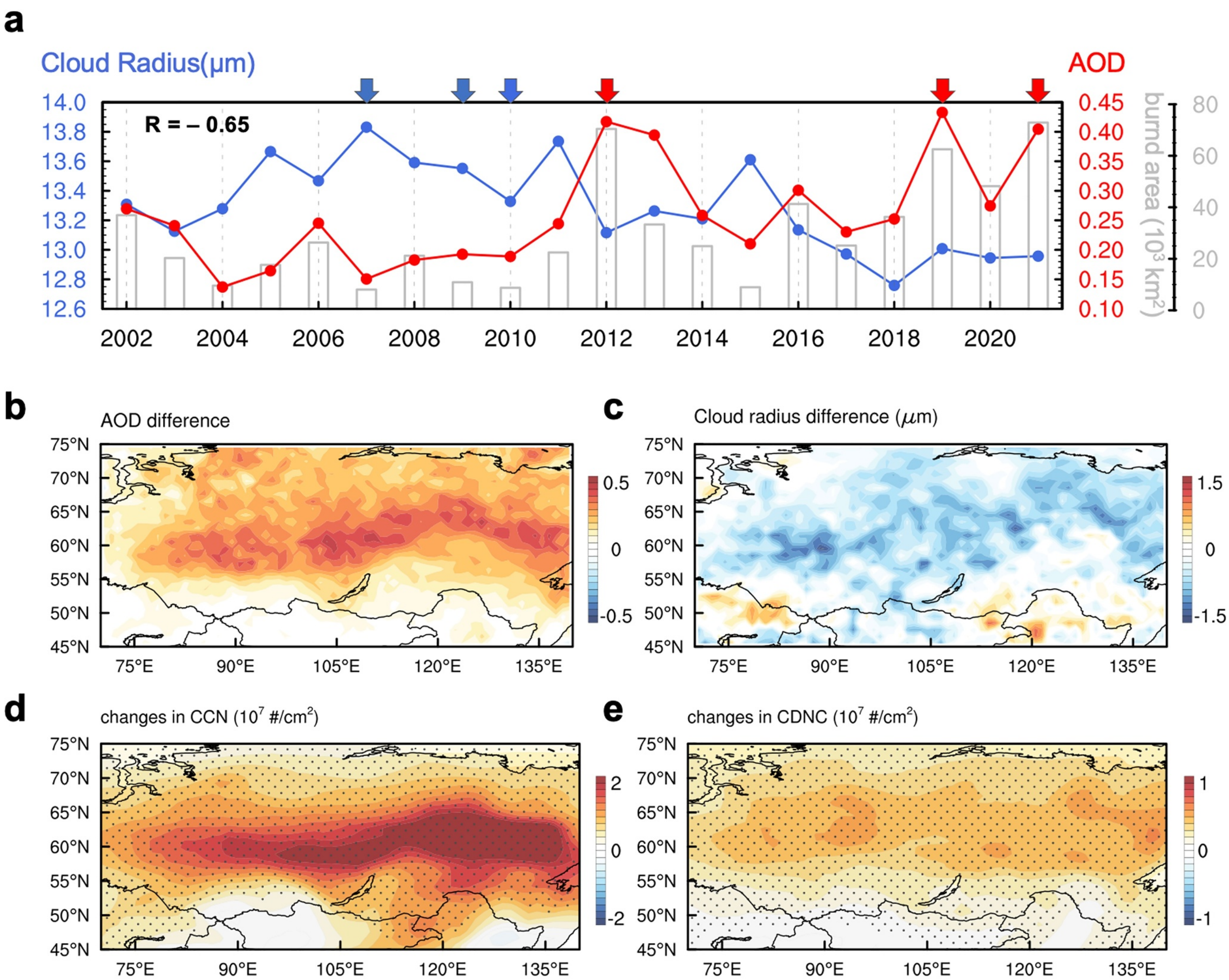

Figure 4. Observed and simulated aerosol-cloud interaction of wildfire smoke. (a) Time series of AOD, burned area and cloud effective radius over central Siberia (black rectangle in Figure 1a) in summer (June–August) derived from MODIS observations (MOD08 version 6.1). The correlation coefficient (R) is labeled in the top left corner. (b) Summertime AOD difference between wildfire-intensive years (red arrows in (a)) and low-fire-severity years (blue arrows in (a)) based on MODIS observations. (c) Same as (b), but for cloud effective radius observations. (d) Summertime responses of column integrated cloud condensation nuclei (CCN) concentration to wildfire smoke aerosols based on CESM climatology simulations with and without wildfire emissions. The gray dots mark areas with statistical significance at the 5% level. (e) Same as (d), but for column-integrated cloud droplet number concentration (CDNC).

contribute to CCN increase (Figure 4d). The model results show that the fire-emitted aerosols could elevate the regional-averaged column CCN number at 0.1% water vapor supersaturation by 39.2% (1.3×10^7 #/cm^2) over central Siberia in summer (Figure 5c).

The summertime cloud base in this region is generally beneath 900 hPa, making itself easily mixed with wildfire smoke aerosols, which is clearly illustrated by both satellite observations and model simulations (Figure S11b in Supporting Information S1). The fire-induced bursting CCN is capable of acting as nuclei for water droplet formation and subsequently perturb the cloud microphysics (Rosenfeld et al., 2014), and thus the cloud droplet number concentration (CDNC) is increased, especially in the fire-intensive region around 60°N (Figure 4e and Figure S12 in Supporting Information S1). Quantitatively, the regional mean column-integrated CDNC almost tripled in response to the CCN increment. Under a certain level of liquid water content in the atmosphere, more CDNC could result in a smaller cloud droplet radius. Accordingly, the regional-mean droplet effective radius declines by 0.4 μm over central Siberia, which is comparable with the decline in cloud radius from satellite observations during the past two decades. A smaller cloud radius thereby inhibits summertime rainfall (Figures 5a and 5b). Sensitivity simulation results indicate that smoke aerosols would induce a decline of almost 8% in

2576604x, 2024, 4, Downloaded from https://agupubs.onlinelibrary.wiley.com/doi/10.1029/2023AV001151 by Nanjing University, Wiley Online Library on [11/09/2024]. See the Terms and Conditions (https://onlinelibrary.wiley.com/terms-and-conditions) on Wiley Online Library for rules of use; OA articles are governed by the applicable Creative Commons License

25766604x, 2024, 4, Downloaded from https://agupubs.onlinelibrary.wiley.com/doi/10.1029/2023AV001151 by Nanjing University, Wiley Online Library on [11/09/2024]. See the Terms and Conditions (https://onlinelibrary.wiley.com/terms-and-conditions) on Wiley Online Library for rules of use; OA articles are governed by the applicable Creative Commons License

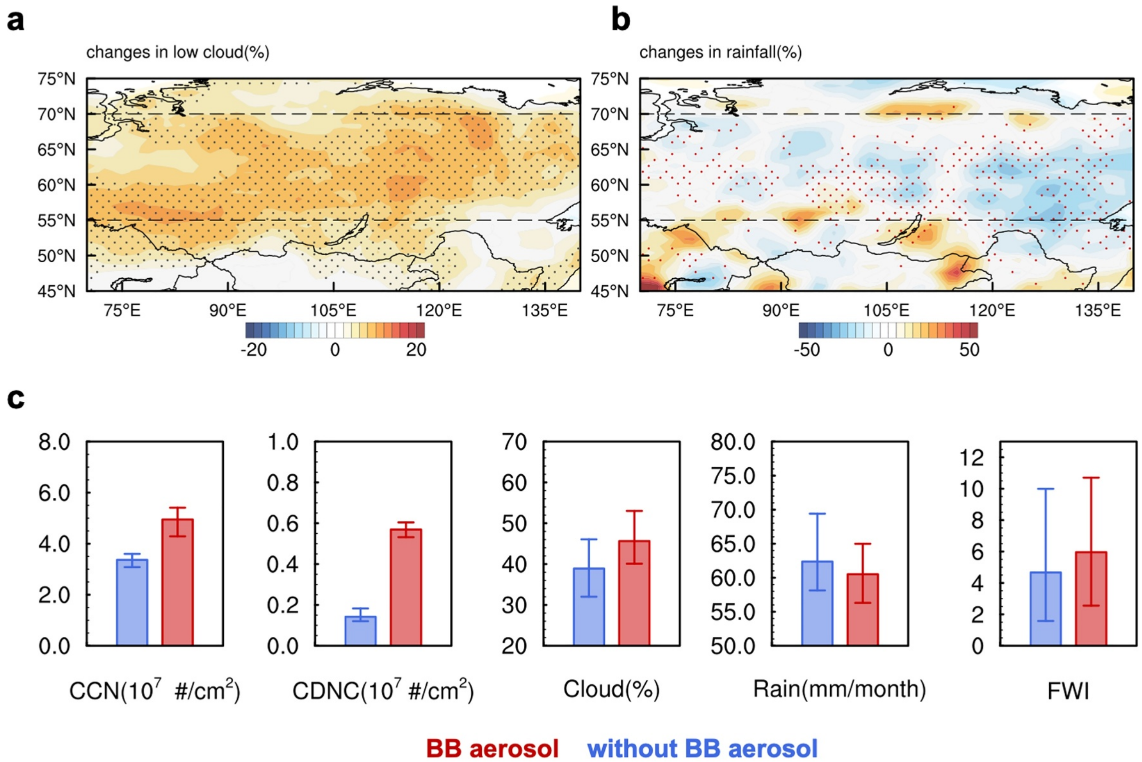

Figure 5. Smoke aerosol-cloud interactions suppress summertime rainfall and amplify fire weather conditions. (a) Responses of summertime low cloud fraction to wildfire smoke aerosols from biomass burning (BB) based on CESM climatology simulations. The gray dots represent areas with statistical significance at the 5% level. (b) Relative changes of summertime rainfall to wildfire smoke aerosols. The red dots mark the fire-prone areas. Dash lines show the central Siberia region for reference. (c) Summer average of column integrated cloud condensation nuclei (CCN) concentration, cloud droplet number concentration (CDNC), low cloud fraction, rainfall rate and fire weather index (FWI) in CESM climatology simulations with and without wildfire emissions. Bars and whiskers show the median values and quartiles, respectively.

summertime rainfall over central Siberia. Such a prominent precipitation suppression is due mainly to the CCN-limited cloud regime and fire-smoke aerosol accumulation (Mauritsen et al., 2011; Petäjä et al., 2022).

In consequence, less rainfall tends to facilitate rigorous and extended hydrological drought, further aggravating the flammability of soil and vegetation. To quantitively understand the responses of fire-prone weather conditions to the smoke aerosol-cloud interactions, the fire weather index (FWI) is calculated based on the CESM simulations with and without fire smoke aerosol (Method and Materials). The FWI is compared with the satellite-detected burned area in Figure S13 in Supporting Information S1, which clearly demonstrates its ability to well characterize the wildfire variations in central Siberia. It is estimated that the regional mean FWI is aggravated by approximately 10% due to the rainfall suppression caused by the fire-emitted smoke aerosol (Figure 5c). Worse still, the FWI increase is extremely distinct in fire-intensive areas, with the maximum value exceeding 40% in the eastern part. It means that, in addition to a warming and drying climate that is fueling Siberian wildfires, smoke aerosols emitted from wildfires could also suppress the rainfall and further dry the soil, which might also play an important role in fire intensification in central Siberia. Wildfire escalation, smoke aerosols, as well as its impacts on cloud and precipitation, have been forming a self-amplifying feedback loop in central Siberia, making wildfire in this region extremely vulnerable to climate change. Such positive feedbacks underscore the fact that increasing wildfire activity is not just a consequence of climate change, but also an active participant.

4. Conclusions and Discussions

Observational evidence and climatology modeling reveal that a warming Arctic and fire self-amplification due to smoke aerosol have been compounding the Siberian wildfire in the past two decades, and central Siberia is identified as a regional "hot spot" for fire poleward expansion and intensification. Given that Arctic warming is very likely to be further escalated in the future, here we apply 20 state-of-the-art global climate simulations under

25766604x, 2024, 4, Downloaded from https://agupubs.onlinelibrary.wiley.com/doi/10.1029/2023AV001151 by Nanjing University, Wiley Online Library on [11/09/2024]. See the Terms and Conditions (https://onlinelibrary.wiley.com/terms-and-conditions) on Wiley Online Library for rules of use; OA articles are governed by the applicable Creative Commons License

different shared socioeconomic pathways, namely SSP1–2.6 and SSP2–4.5 from CMIP6 (SI Materials and Methods), to characterize the fire regime and its potential changes by mid- and late 21st century (Figure S14 in Supporting Information S1). Arctic is projected to be further warmed by 4.7 ± 0.9°C and 7.6 ± 1.1°C around 2100, with the summer warming in central Siberia by 4.7 ± 0.1°C and 4.8 ± 0.2°C under SSP1–2.6 and SSP2–4.5 pathways, respectively.

The future warming could further reduce the soil water storage at high latitudes in the Arctic circumpolar region with higher vapor pressure deficit (Dai et al., 2018; Zhang et al., 2021). Furthermore, a weaker and pole-ward-shifted jet stream under a warming Arctic may substantially increase the risk of concurrent extreme droughts and heat waves, potentially drying out the soil (Zscheischler & Seneviratne, 2017). As illustrated, the soil moisture in central Siberia at the end of this century is subject to a decline of ∼28% and ∼39% under SSP1–2.6 and SSP2–4.5 pathways, respectively. On the basis of the correlation of fire intensity with soil moisture, the fire severity over this region is predicted to increase by 200%–350% by the end of the 21st century. Such fire intensification and poleward expansion might be even more pronounced since the increasing lightning frequency is expected to further compound the fire escalation in Siberia (Chen et al., 2021). Even worse, under Arctic warming in the future, the deposition of fire-emitted carbonaceous aerosol may accelerate snow melting and increase fire frequency in what had traditionally been a low flammability landscape (You & Xu, 2022), presenting new challenges for fire management and climate adaptation in Siberia.

Conflict of Interest

The authors declare no conflicts of interest relevant to this study.

Data Availability Statement

FINN wildfire emissions data is openly accessible at https://www.acom.ucar.edu/Data/fire (Wiedinmyer et al., 2011). MODIS thermal anomalies/Fire products are available at https://lpdaac.usgs.gov/products/mod14a1v061/ (Giglio and Justice, 2021). ERA5 atmospheric reanalysis is openly accessible at https://cds.climate.copernicus.eu/cdsapp#!/dataset/reanalysis-era5-single-levels (Hersbach et al., 2023). Permafrost map are obtained from https://climate.esa.int/en/projects/permafrost/data (Westermann et al., 2024). Surface hourly temperature observations are archived at https://rda.ucar.edu/datasets/ds463.3 (Air Force Combat Climatology Center/U.S. Air Force/U.S. Department of Defense557th Weather Wing/U.S. Air Force/U. S. Department of Defenseand National Climatic Data Center/NESDIS/NOAA/U.S. Department of Commerce, 2005). The fire weather index data set is obtained from https://cds.climate.copernicus.eu/cdsapp#!/dataset/cems-fire-historical (Copernicus Climate Change Service and Climate Data Store, 2019).

Acknowledgments
This work was supported by the National Natural Science Foundation of China (42325506, 42105095, and 41922038), the Fundamental Research Funds for the Central Universities in China (14380187), and Jiangsu Natural Science Foundation (BK20210197).

References

Abatzoglou, J. T., Rupp, D. E., O'Neill, L. W., & Sadegh, M. (2021). Compound extremes drive the western Oregon wildfires of September 2020. *Geophysical Research Letters*, *48*(8), e2021GL092520. https://doi.org/10.1029/2021GL092520

Air Force Combat Climatology Center/U.S. Air Force/U.S. Department of Defense, 557th Weather Wing/U.S. Air Force/U. S. Department of Defense, and National Climatic Data Center/NESDIS/NOAA/U.S. Department of Commerce. (2005). NCDC TD3505 integrated surface hourly data [Dataset]. *Research Data Archive at the National Center for Atmospheric Research, Computational and Information Systems Laboratory*. Retrieved from https://rda.ucar.edu/datasets/ds463.3/

Aubry-Wake, C., Bertoncini, A., & Pomeroy, J. W. (2022). Fire and ice: The impact of wildfire-affected albedo and irradiance on glacier melt. *Earth's Future*, *10*(4), e2022EF002685. https://doi.org/10.1029/2022EF002685

Baklanov, A., Chew, B. N., Frassoni, A., Gan, C., Goldammer, J., Keywood, M., et al. (2021). The WMO vegetation fire and smoke pollution warning advisory and assessment system (VFSP-WAS): Concept, current capabilities, research and development challenges and the way ahead. *Biodiversidade Brasileira - BioBrasil*, *11*(2), 179–201. https://doi.org/10.37002/biobrasil.v11i2.1738

Bartsch, A., Balzter, H., & George, C. (2009). The influence of regional surface soil moisture anomalies on forest fires in Siberia observed from satellites. *Environmental Research Letters*, *4*(4), 045021. https://doi.org/10.1088/1748-9326/4/4/045021

Bessie, W. C., & Johnson, E. A. (1995). The relative importance of fuels and weather on fire behavior in subalpine forests. *Ecology*, *76*(3), 747–762. https://doi.org/10.2307/1939341

Bond-Lamberty, B., Peckham, S. D., Ahl, D. E., & Gower, S. T. (2007). Fire as the dominant driver of central Canadian boreal forest carbon balance. *Nature*, *450*(7166), 89–92. https://doi.org/10.1038/nature06272

Brown, P. T., Hanley, H., Mahesh, A., Reed, C., Strenfel, S. J., Davis, S. J., et al. (2023). Climate warming increases extreme daily wildfire growth risk in California. *Nature*, *621*(7980), 760–766. https://doi.org/10.1038/s41586-023-06444-3

Chen, Y., Romps, D. M., Seeley, J. T., Veraverbeke, S., Riley, W. J., Mekonnen, Z. A., & Randerson, J. T. (2021). Future increases in Arctic lightning and fire risk for permafrost carbon. *Nature Climate Change*, *11*(5), 404–410. https://doi.org/10.1038/s41558-021-01011-y

Copernicus Climate Change Service, Climate Data Store. (2019). Fire danger indices historical data from the Copernicus Emergency Management Service [Dataset]. *Copernicus Climate Change Service (C3S) Climate Data Store (CDS)*. https://doi.org/10.24381/cds.0e89c522

25766604x, 2024, 4, Downloaded from https://agupubs.onlinelibrary.wiley.com/doi/10.1029/2023AV001151 by Nanjing University, Wiley Online Library on [11/09/2024]. See the Terms and Conditions (https://onlinelibrary.wiley.com/terms-and-conditions) on Wiley Online Library for rules of use; OA articles are governed by the applicable Creative Commons License

Coumou, D., Lehmann, J., & Beckmann, J. (2015). The weakening summer circulation in the Northern Hemisphere mid-latitudes. *Science*, *348*(6232), 324–327. https://doi.org/10.1126/science.1261768

Dai, A., Zhao, T., & Chen, J. (2018). Climate change and drought: A precipitation and evaporation perspective. *Current Climate Change Reports*, *4*(3), 301–312. https://doi.org/10.1007/s40641-018-0101-6

Danabasoglu, G., Lamarque, J. F., Bacmeister, J., Bailey, D. A., DuVivier, A. K., Edwards, J., et al. (2020). The Community Earth System Model Version 2 (CESM2). *Journal of Advances in Modeling Earth Systems*, *12*(2), e2019MS001916. https://doi.org/10.1029/2019MS001916

Descals, A., Gaveau, D. L. A., Verger, A., Sheil, D., Naito, D., & Peñuelas, J. (2022). Unprecedented fire activity above the Arctic Circle linked to rising temperatures. *Science*, *378*(6619), 532–537. https://doi.org/10.1126/science.abn9768

Francis, J. A., Vavrus, S. J., & Cohen, J. (2017). Amplified Arctic warming and mid-latitude weather: New perspectives on emerging connections. *Wiley Interdisciplinary Reviews: Climate Change*, *8*(5). https://doi.org/10.1002/wcc.474

Fukutomi, Y., Masuda, K., & Yasunari, T. (2004). Role of storm track activity in the interannual seesaw of summer precipitation over northern Eurasia. *Journal of Geophysical Research*, *109*(2), 2109. https://doi.org/10.1029/2003jd003912

Gao, M., Ji, D., Liang, F., & Liu, Y. (2018). Attribution of aerosol direct radiative forcing in China and India to emitting sectors. *Atmospheric Environment*, *190*, 35–42. https://doi.org/10.1016/j.atmosenv.2018.07.011

Giglio, L., & Justice, C. (2021). MODIS/Terra thermal anomalies/fire daily L3 global 1km SIN grid V061 [Dataset]. *NASA EOSDIS Land Processes Distributed Active Archive Center*. https://doi.org/10.5067/MODIS/MOD14A1.061

Giglio, L., Randerson, J. T., & Van Der Werf, G. R. (2013). Analysis of daily, monthly, and annual burned area using the fourth-generation global fire emissions database (GFED4). *Journal of Geophysical Research: Biogeosciences*, *118*(1), 317–328. https://doi.org/10.1002/jgrg.20042

Guan, S., Wong, D. C., Gao, Y., Zhang, T., & Pouliot, G. (2020). Impact of wildfire on particulate matter in the southeastern United States in November 2016. *Science of the Total Environment*, *724*, 138354. https://doi.org/10.1016/j.scitotenv.2020.138354

Hersbach, H., Bell, B., Berrisford, P., Biavati, G., Horányi, A., Muñoz Sabater, J., et al. (2023). ERA5 hourly data on single levels from 1940 to present [Dataset]. *Copernicus Climate Change Service (C3S) Climate Data Store (CDS)*. https://doi.org/10.24381/cds.adbb2d47

Hoesly, R. M., Smith, S. J., Feng, L., Klimont, Z., Janssens-Maenhout, G., Pitkanen, T., et al. (2018). Historical (1750-2014) anthropogenic emissions of reactive gases and aerosols from the Community Emissions Data System (CEDS). *Geoscientific Model Development*, *11*(1), 369–408. https://doi.org/10.5194/gmd-11-369-2018

Hoskins, B., & Woollings, T. (2015). Persistent extratropical regimes and climate extremes. *Current Climate Change Reports*, *1*(3), 115–124. https://doi.org/10.1007/s40641-015-0020-8

Hu, Y., Fernandez-Anez, N., Smith, T. E. L., & Rein, G. (2018). Review of emissions from smouldering peat fires and their contribution to regional haze episodes. *International Journal of Wildland Fire*, *27*(5), 293–312. https://doi.org/10.1071/WF17084

Huang, J., Zhang, X., Zhang, Q., Lin, Y., Hao, M., Luo, Y., et al. (2017). Recently amplified arctic warming has contributed to a continual global warming trend. *Nature Climate Change*, *7*(12), 875–879. https://doi.org/10.1038/s41558-017-0009-5

Huang, X., Ding, K., Liu, J., Wang, Z., Tang, R., Xue, L., et al. (2023). Smoke-weather interaction affects extreme wildfires in diverse coastal regions. *Science*, *379*(6631), 457–461. https://doi.org/10.1126/science.add9843

Hugelius, G., Strauss, J., Zubrzycki, S., Harden, J. W., Schuur, E. A. G., Ping, C. L., et al. (2014). Estimated stocks of circumpolar permafrost carbon with quantified uncertainty ranges and identified data gaps. *Biogeosciences*, *11*(23), 6573–6593. https://doi.org/10.5194/bg-11-6573-2014

Irannezhad, M., Liu, J., Ahmadi, B., & Chen, D. (2020). The dangers of Arctic zombie wildfires. *Science*, *369*(6508), 1171. https://doi.org/10.1126/SCIENCE.ABE1739

Jones, M. W., Abatzoglou, J. T., Veraverbeke, S., Andela, N., Lasslop, G., Forkel, M., et al. (2022). Global and regional trends and drivers of fire under climate change. *Reviews of Geophysics*, *60*(3), e2020RG000726. https://doi.org/10.1029/2020RG000726

Kim, J. S., Kug, J. S., Jeong, S. J., Park, H., & Schaepman-Strub, G. (2020). Extensive fires in southeastern Siberian permafrost linked to preceding Arctic Oscillation. *Science Advances*, *6*(2). https://doi.org/10.1126/sciadv.aax3308

Kirillina, K., Shvetsov, E. G., Protopopova, V. V., Thiesmeyer, L., & Yan, W. (2020). Consideration of anthropogenic factors in boreal forest fire regime changes during rapid socio-economic development: Case study of forestry districts with increasing burnt area in the Sakha Republic, Russia. *Environmental Research Letters*, *15*(3), 035009. https://doi.org/10.1088/1748-9326/ab6c6e

Kochanski, A. K., Mallia, D. V., Fearon, M. G., Mandel, J., Souri, A. H., & Brown, T. (2019). Modeling wildfire smoke feedback mechanisms using a coupled fire-atmosphere model with a radiatively active aerosol scheme. *Journal of Geophysical Research: Atmospheres*, *124*(16), 9099–9116. https://doi.org/10.1029/2019JD030558

Liu, X., Ma, P. L., Wang, H., Tilmes, S., Singh, B., Easter, R. C., et al. (2016). Description and evaluation of a new four-mode version of the Modal Aerosol Module (MAM4) within version 5.3 of the Community Atmosphere Model. *Geoscientific Model Development*, *9*(2), 505–522. https://doi.org/10.5194/gmd-9-505-2016

Liu, Y., Stanturf, J., & Goodrick, S. (2010). Trends in global wildfire potential in a changing climate. *Forest Ecology and Management*, *259*(4), 685–697. https://doi.org/10.1016/j.foreco.2009.09.002

Lu, Z., Liu, X., Zhang, Z., Zhao, C., Meyer, K., Rajapakshe, C., et al. (2018). Biomass smoke from southern Africa can significantly enhance the brightness of stratocumulus over the southeastern Atlantic Ocean. *Proceedings of the National Academy of Sciences of the United States of America*, *115*(12), 2924–2929. https://doi.org/10.1073/pnas.1713703115

Marquardt Collow, A. B., Thomas, N. P., Bosilovich, M. G., Lim, Y. K., Schubert, S. D., & Koster, R. D. (2022). Seasonal variability in the mechanisms behind the 2020 Siberian Heatwaves. *Journal of Climate*, *35*(10), 3075–3090. https://doi.org/10.1175/JCLI-D-21-0432.1

Masrur, A., Petrov, A. N., & DeGroote, J. (2018). Circumpolar spatio-temporal patterns and contributing climatic factors of wildfire activity in the Arctic tundra from 2001-2015. *Environmental Research Letters*, *13*(1), 14019. https://doi.org/10.1088/1748-9326/aa9a76

Mauritsen, T., Sedlar, J., TjernstrÃm, M., Leck, C., Martin, M., Shupe, M., et al. (2011). An Arctic CCN-limited cloud-aerosol regime. *Atmospheric Chemistry and Physics*, *11*(1), 165–173. https://doi.org/10.5194/acp-11-165-2011

Mccarty, J. L., Aalto, J., Paunu, V. V., Arnold, S. R., Eckhardt, S., Klimont, Z., et al. (2021). Reviews and syntheses: Arctic fire regimes and emissions in the 21st century. *Biogeosciences*, *18*(18), 5053–5083. https://doi.org/10.5194/bg-18-5053-2021

McCarty, J. L., Smith, T. E. L., & Turetsky, M. R. (2020). Arctic fires re-emerging. *Nature Geoscience*, *13*(10), 658–660. https://doi.org/10.1038/s41561-020-00645-5

Mekonnen, Z. A., Riley, W. J., Randerson, J. T., Shirley, I. A., Bouskill, N. J., & Grant, R. F. (2022). Wildfire exacerbates high-latitude soil carbon losses from climate warming. *Environmental Research Letters*, *17*(9), 094037. https://doi.org/10.1088/1748-9326/AC8BE6

Miner, K. R., Turetsky, M. R., Malina, E., Bartsch, A., Tamminen, J., McGuire, A. D., et al. (2022). Permafrost carbon emissions in a changing Arctic. *Nature Reviews Earth & Environment*, *3*(1), 55–67. https://doi.org/10.1038/s43017-021-00230-3

Nitzbon, J., Westermann, S., Langer, M., Martin, L. C. P., Strauss, J., Laboor, S., & Boike, J. (2020). Fast response of cold ice-rich permafrost in northeast Siberia to a warming climate. *Nature Communications*, *11*(1), 2201. https://doi.org/10.1038/s41467-020-15725-8

Obu, J., Westermann, S., Barboux, C., Bartsch, A., Delaloye, R., Grosse, G., et al. (2021). ESA permafrost climate change initiative (Permafrost_cci): Permafrost active layer thickness for the Northern Hemisphere, v3.0. Retrieved from https://catalogue.ceda.ac.uk/uuid/6e2091cb0c8b4106921b63cd5357c97c

Pan, Y., Birdsey, R. A., Fang, J., Houghton, R., Kauppi, P. E., Kurz, W. A., et al. (2011). A large and persistent carbon sink in the world's forests. *Science*, *333*(6045), 988–993. https://doi.org/10.1126/science.1201609

Petäjä, T., Järvi, L., Kerminen, V.-M., Ding, A. J., Sun, J. N., Nie, W., et al. (2016). Enhanced air pollution via aerosol-boundary layer feedback in China. *Scientific Reports*, *6*(1), 18998. https://doi.org/10.1038/srep18998

Petäjä, T., Tabakova, K., Manninen, A., Ezhova, E., O'Connor, E., Moisseev, D., et al. (2022). Influence of biogenic emissions from boreal forests on aerosol–cloud interactions. *Nature Geoscience*, *15*(1), 42–47. https://doi.org/10.1038/s41561-021-00876-0

Piao, J., Chen, W., Chen, S., Gong, H., & Zhang, Q. (2020). Summer water vapor Sources in Northeast Asia and East Siberia revealed by a moisture-tracing atmospheric model. *Journal of Climate*, *33*(9), 3883–3899. https://doi.org/10.1175/JCLI-D-19-0516.1

Post, E., Alley, R. B., Christensen, T. R., Macias-Fauria, M., Forbes, B. C., Gooseff, M. N., et al. (2019). The polar regions in a 2°C warmer world. *Science Advances*, *5*(12). https://doi.org/10.1126/sciadv.aaw9883

Rein, G. (2013). Smouldering fires and natural fuels. In *Fire phenomena and the Earth system: An interdisciplinary guide to fire science* (pp. 15–33). https://doi.org/10.1002/9781118529539.ch2

Rein, G., & Huang, X. (2021). Smouldering wildfires in peatlands, forests and the arctic: Challenges and perspectives. *Current Opinion in Environmental Science and Health*, *24*, 100296. https://doi.org/10.1016/j.coesh.2021.100296

Rosenfeld, D., Andreae, M. O., Asmi, A., Chin, M., De Leeuw, G., Donovan, D. P., et al. (2014). Global observations of aerosol-cloud-precipitation-climate interactions. *Reviews of Geophysics*, *52*(4), 750–808. https://doi.org/10.1002/2013RG000441

Schill, G. P., Froyd, K. D., Bian, H., Kupc, A., Williamson, C., Brock, C. A., et al. (2020). Widespread biomass burning smoke throughout the remote troposphere. *Nature Geoscience*, *13*(6), 422–427. https://doi.org/10.1038/s41561-020-0586-1

Scholten, R. C., Coumou, D., Luo, F., & Veraverbeke, S. (2022). Early snowmelt and polar jet dynamics co-influence recent extreme Siberian fire seasons. *Science*, *378*(6623), 1005–1009. https://doi.org/10.1126/science.abn4419

Schuur, E. A. G., McGuire, A. D., Schädel, C., Grosse, G., Harden, J. W., Hayes, D. J., et al. (2015). Climate change and the permafrost carbon feedback. *Nature*, *520*(7546), 171–179. https://doi.org/10.1038/nature14338

Serreze, M. C., Bromwich, D. H., Clark, M. P., Etringer, A. J., Zhang, T., & Lammers, R. (2003). Large-scale hydro-climatology of the terrestrial Arctic drainage system. *Journal of Geophysical Research: Atmospheres*, *108*(2), ALT1-1–ALT1-28. https://doi.org/10.1029/2001JD000919

Smith, A. J. P., Smith, D. M., Cohen, J., & Jones, M. W. (2021). Arctic warming amplifies climate change and its impacts. *Science Review*.

Song, J., Liu, Z., Zhang, Y., Yan, T., Shen, Z., & Piao, S. (2019). Effects of wildfire on soil respiration and its heterotrophic and autotrophic components in a montane coniferous forest. *Journal of Plant Ecology*, *12*(2), 336–345. https://doi.org/10.1093/jpe/rty031

Stevens, R. G., Loewe, K., Dearden, C., Dimitrelos, A., Possner, A., Eirund, G. K., et al. (2018). A model intercomparison of CCN-limited tenuous clouds in the high Arctic. *Atmospheric Chemistry and Physics*, *18*(15), 11041–11071. https://doi.org/10.5194/acp-18-11041-2018

Talucci, A. C., Loranty, M. M., & Alexander, H. D. (2022). Siberian taiga and tundra fire regimes from 2001-2020. *Environmental Research Letters*, *17*(2), 025001. https://doi.org/10.1088/1748-9326/ac3f07

Tomshin, O., & Solovyev, V. (2021). Spatio-temporal patterns of wildfires in Siberia during 2001–2020. *Geocarto International*, *37*(25), 7339–7357. https://doi.org/10.1080/10106049.2021.1973581

Van Marle, M. J. E., Kloster, S., Magi, B. I., Marlon, J. R., Daniau, A. L., Field, R. D., et al. (2017). Historic global biomass burning emissions for CMIP6 (BB4CMIP) based on merging satellite observations with proxies and fire models (1750-2015). *Geoscientific Model Development*, *10*(9), 3329–3357. https://doi.org/10.5194/gmd-10-3329-2017

Van Wagner, C. E. (1987). Development and structure of the Canadian forest fire weather index system. In *Forestry* (Vol. 35). Canadian Forestry Service.

Walker, X. J., Baltzer, J. L., Cumming, S. G., Day, N. J., Ebert, C., Goetz, S., et al. (2019). Increasing wildfires threaten historic carbon sink of boreal forest soils. *Nature*, *572*(7770), 520–523. https://doi.org/10.1038/s41586-019-1474-y

Westerling, A. L., Hidalgo, H. G., Cayan, D. R., & Swetnam, T. W. (2006). Warming and earlier spring increase Western U.S. forest wildfire activity. *Science*, *313*(5789), 940–943. https://doi.org/10.1126/science.1128834

Westermann, S., Barboux, C., Bartsch, A., Delaloye, R., Grosse, G., Heim, B., et al. (2024). ESA permafrost climate change initiative (Permafrost_cci). Permafrost version 4 data products [Dataset]. *NERC EDS Centre for Environmental Data Analysis*. http://catalogue.ceda.ac.uk/uuid/7479606004d9465bad949671501e5f21

Wiedinmyer, C., Akagi, S. K., Yokelson, R. J., Emmons, L. K., Al-Saadi, J. A., Orlando, J. J., & Soja, A. J. (2011). The Fire INventory from NCAR (FINN): A high resolution global model to estimate the emissions from open burning. *Geoscientific Model Development*, *4*(3), 625–641. https://doi.org/10.5194/gmd-4-625-2011

Xing, C., Liu, C., Wang, S., Lok Chan, K., Gao, Y., Huang, X., et al. (2017). Observations of the vertical distributions of summertime atmospheric pollutants and the corresponding ozone production in Shanghai, China. *Atmospheric Chemistry and Physics*, *17*(23), 14275–14289. https://doi.org/10.5194/acp-17-14275-2017

Xu, P., Wang, L., & Chen, W. (2019). The British-Baikal Corridor: A teleconnection pattern along the summertime polar front jet over Eurasia. *Journal of Climate*, *32*(3), 877–896. https://doi.org/10.1175/JCLI-D-18-0343.1

You, C., & Xu, C. (2022). Himalayan glaciers threatened by frequent wildfires. *Nature Geoscience 2022*, *15*(12), 956–957. https://doi.org/10.1038/s41561-022-01076-0

Yu, P., Toon, O. B., Bardeen, C. G., Zhu, Y., Rosenlof, K. H., Portmann, R. W., et al. (2019). Black carbon lofts wildfire smoke high into the stratosphere to form a persistent plume. *Science*, *365*(6453), 587–590. https://doi.org/10.1126/science.aax1748

Zhang, Y., Ma, N., Park, H., Walsh, J. E., & Zhang, K. (2021). Evaporation processes and changes over the Northern Regions. *Arctic Hydrology, Permafrost and Ecosystems*, 101–131. https://doi.org/10.1007/978-3-030-50930-9_4

Zheng, B., Ciais, P., Chevallier, F., Chuvieco, E., Chen, Y., & Yang, H. (2021). Increasing forest fire emissions despite the decline in global burned area. *Science Advances*, *7*(39). https://doi.org/10.1126/sciadv.abh2646

Zheng, B., Ciais, P., Chevallier, F., Yang, H., Canadell, J. G., Chen, Y., et al. (2023). Record-high CO_2 emissions from boreal fires in 2021. *Science*, *379*(6635), 912–917. https://doi.org/10.1126/SCIENCE.ADE0805/SUPPL_FILE/SCIENCE.ADE0805_SM.PDF

Zhu, X., Xu, X., & Jia, G. (2021). Asymmetrical trends of burned area between eastern and western Siberia regulated by atmospheric oscillation. *Geophysical Research Letters*, *48*(24), e2021GL096095. https://doi.org/10.1029/2021GL096095

Zscheischler, J., & Seneviratne, S. I. (2017). Dependence of drivers affects risks associated with compound events. *Science Advances*, *3*(6). https://doi.org/10.1126/sciadv.1700263

2576604x, 2024, 4, Downloaded from https://agupubs.onlinelibrary.wiley.com/doi/10.1029/2023AV001151 by Nanjing University, Wiley Online Library on [11/09/2024]. See the Terms and Conditions (https://onlinelibrary.wiley.com/terms-and-conditions) on Wiley Online Library for rules of use; OA articles are governed by the applicable Creative Commons License

References From the Supporting Information

Eyring, V., Bony, S., Meehl, G. A., Senior, C. A., Stevens, B., Stouffer, R. J., & Taylor, K. E. (2016). Overview of the Coupled Model Intercomparison Project Phase 6 (CMIP6) experimental design and organization. *Geoscientific Model Development*, *9*(5), 1937–1958. https://doi.org/10.5194/gmd-9-1937-2016

He, B., Bao, Q., Wang, X., Zhou, L., Wu, X., Liu, Y., et al. (2019). CAS FGOALS-f3-L model datasets for CMIP6 historical atmospheric model intercomparison project simulation. *Advances in Atmospheric Sciences*, *36*(8), 771–778. https://doi.org/10.1007/s00376-019-9027-8

Lauritzen, P. H., Nair, R. D., Herrington, A. R., Callaghan, P., Goldhaber, S., Dennis, J. M., et al. (2018). NCAR release of CAM-SE in CESM2.0: A reformulation of the spectral element dynamical core in dry-mass vertical coordinates with comprehensive treatment of condensates and energy. *Journal of Advances in Modeling Earth Systems*, *10*(7), 1537–1570. https://doi.org/10.1029/2017MS001257

Oshima, K., & Yamazaki, K. (2006). Difference in seasonal variation of net precipitation between the Arctic and Antarctic regions. *Geophysical Research Letters*, *33*(18), L18501. https://doi.org/10.1029/2006GL027389

Sellar, A. A., Jones, C. G., Mulcahy, J. P., Tang, Y., Yool, A., Wiltshire, A., et al. (2019). UKESM1: Description and evaluation of the U.K. Earth system model. *Journal of Advances in Modeling Earth Systems*, *11*(12), 4513–4558. https://doi.org/10.1029/2019MS001739

Tatebe, H., Ogura, T., Nitta, T., Komuro, Y., Ogochi, K., Takemura, T., et al. (2019). Description and basic evaluation of simulated mean state, internal variability, and climate sensitivity in MIROC6. *Geoscientific Model Development*, *12*(7), 2727–2765. https://doi.org/10.5194/gmd-12-2727-2019

Winker, D. M., Pelon, J. R., & McCormick, M. P. (2003). The CALIPSO mission: Spaceborne lidar for observation of aerosols and clouds. *Lidar Remote Sensing for Industry and Environment Monitoring III*, *4893*, 1. https://doi.org/10.1117/12.466539

Wu, T., Lu, Y., Fang, Y., Xin, X., Li, L., Li, W., et al. (2019). The Beijing Climate Center Climate System Model (BCC-CSM): The main progress from CMIP5 to CMIP6. *Geoscientific Model Development*, *12*(4), 1573–1600. https://doi.org/10.5194/gmd-12-1573-2019

Yao, P., Lu, H., Shi, J., Zhao, T., Yang, K., Cosh, M. H., et al. (2021). A long term global daily soil moisture dataset derived from AMSR-E and AMSR2 (2002–2019). *Scientific Data*, *8*(1), 1–16. https://doi.org/10.1038/s41597-021-00925-8

2576604x, 2024, 4, Downloaded from https://agupubs.onlinelibrary.wiley.com/doi/10.1029/2023AV001151 by Nanjing University, Wiley Online Library on [11/09/2024]. See the Terms and Conditions (https://onlinelibrary.wiley.com/terms-and-conditions) on Wiley Online Library for rules of use; OA articles are governed by the applicable Creative Commons License